arXiv:1605.02853v1 [quant-ph] 10 May 2016

Practical decoy-state round-robin differential-phase-shift quantum key distribution

Ying-Ying Zhang[1,2], Wan-Su Bao[1,2,⋆], Chun Zhou[1,2], Hong-Wei Li[1,2], Yang Wang[1,2], Mu-Sheng Jiang[1,2]

[1] *Zhengzhou Information Science and Technology Institute, Zhengzhou, 450001, China*

[2] *Synergetic Innovation Center of Quantum Information & Quantum Physics, University of Science and Technology of China, Hefei, 230026, China*

⋆ *e-mail:2010thzz@sina.com.*

To overcome the signal disturbance from the transmission process, recently, a new type of protocol named round-robin differential-phase-shift(RRDPS) quantum key distribution[Nature 509, 475(2014)] is proposed. It can estimate how much information has leaked to eavesdropper without monitoring bit error rates. In this paper, we compare the performance of RRDPS using different sources without and with decoy-state method, such as weak coherent pulses(WCPs) and heralded single photon source(HSPS). For practical implementations, we propose finite decoy-state method for RRDPS, the performance of which is close to the infinite one. Taking WCPs as an example, the three-intensity decoy-state protocol can distribute secret keys over a distance of 128 km when the length of pulses packet is 32, which confirms the great practical interest of our method.

Introduction

Quantum key distribution(QKD)[1,2] enables two legitimate communication participants, Alice and Bob, to share identical keys based on the fundamental laws of quantum physics. It has been a kind of information security technology raised from modern cryptography and quantum mechanics. QKD can be considered the most important application of quantum physics. Many papers have proven the security of Bennett-Brassard-1984(BB84) protocol[3,4]. Subsequently the experimental implementation also made great progress[5–7]. So far, commercial products have already become available. However, due to the symmetry of BB84 protocol, the phase error rate is equal to the bit error rate. Needing to estimate the amount of leaked information by randomly sampling the signal, BB84 protocol may overestimate the leaked information and limit the threshold of the error rate.

Recently, a quantum key distribution protocol called round-robin differential phase-shift(RRDPS) was proposed by Sasaki et al.[8], which can generate keys without monitoring signal disturbance of the measurement outcomes and has no restriction on the error rate[9]. RRDPS is a novel method to encode raw key bits even with the existence of eavesdropper, in which Bob specifies randomly how to calculate the sifted key from the raw key bits. Due to the large number of pulses in a packet, RRDPS system has higher stability and lower loss. It can tolerate a noisier channel than the conventional one. Up to now, many modified schemes have been proposed and several experimental demonstrations have been performed[10–13]. Using a receiver set-up to randomly choose one of four interferometers with different delays, Takesue et al.[10] reported a proof-of-principle QKD experiment based on RRDPS protocol. Wang et al.[11] demonstrated an active implementation of this protocol, and their system can distribute secret keys over a distance of 90 km. Implementation results show that the protocol is feasible with current tech-

nology, especially in high-error situations[11].

Similar to the standard QKD protocol, most researches of RRDPS use weak coherent pulses(WCPs) as a replacement of the perfect single-photon source. Heralded single photon source (HSPS), is also within reach of current technology and can be considered as the candidate of the perfect single-photon source. So the performance of this source in RRDPS remains to be further studied.

In BB84 protocol, decoy-state method[14–17] can be used to efficiently estimate the contribution of the single-photon pulse and significantly increase the transmission distance of secure keys. Many researchers have studied the practicability of decoy-state method. Ma et al. [17] first studied the statistical fluctuation analysis for the decoy state. Similarly, Zhang et al.[9] proposed the infinite decoy-state method for RRDPS. Their method is valid in the asymptotic limit with an infinite number of decoy states, thus it has some limitations in practice. We extend it to the practical case with a finite number of decoy states.

First of all, we compare the performance of WCPs and HSPS in different pulse packet lengths. Then, fixing the packet length at 32, we simulate the infinite decoy-state method using these two sources. Since infinite decoy-state method is difficult to achieve in practice, we put forward a finite decoy-state protocol. Taking WCPs as an example, bounds on the yields and quantum bit error rates of some photon number states are stated. At last, considering that contributions from three and more photons are not obvious, we employ three-intensity decoy-state method.

Results

Round-robin differential-phase-shift protocol

The round-robin differential-phase-shift protocol encodes raw key bits coherently so that only a few bits can be read out at the same time. It is hard for Eve to guess the sifted key. The ideal protocol, between two legitimate users, Alice and Bob, runs as follows.

1. State Preparation. Alice prepares packets of pulses containing L pulses, and generates a random L-bit sequence, $s = (s_1, s_2, \cdots, s_L)$. Then she encodes the sequence into the phase of each pulse, 0(when $s_i = 0$) or π(when $s_i = 1$), and sends the pulse packets to Bob. We consider that the encoded signal is a superposition photon state of pulses[8]

$$|\psi >= \frac{1}{\sqrt{L}} \sum_{k=1}^{L} (-1)^{s_k} |k > \tag{1}$$

where s_k is the encoded bit sequence, $|k >$ denotes that the photon is in the k-th pulse.

2. Measurement. Upon receiving the states, Bob randomly sets the pulse delay value $r(1 \leq r \leq L-1)$, and splits each received L-pulse train into two. Then Bob delays one of the train and interferes with the other. After measuring interference between the two trains, the detection result shows the phase difference between two pulses i and$j$ $(\{i, j\} \subset \{1, 2, \cdots L\})$ satisfying $j - i = \pm r(\mathrm{mod} L)$. The value of the relative phase $s_B = s_i \oplus s_j$ is a sifted key of Bob.

3. Sifting. Bob announces $\{i, j\}$ to Alice through classical channel, so that Alice computes $s_A = s_i \oplus s_j$ as her sifted key.

4. Post Processing. Alice and Bob repeat steps 1-3 to accumulate enough sifted key. They

perform error correction and privacy amplification on the sifted key to extract the final secure key.

The sketch of the protocol is shown in the Figure 1.

[ht]

The secure key length of QKD protocol is given by [4]

$$G = N[1 - f \cdot h(e_{bit}) - h(e_{phase})] \tag{2}$$

where N is the sifted key length, f corresponds to the efficiency of error correction, and $h(e) = -e \log e - (1-e)\log(1-e)$ is the binary Shannon entropy function. Moreover, e_{bit} and e_{phase} are the bit error rate and phase error rate respectively.

As for RRDPS protocol, the phase error rate depends on the preparation of quantum states rather than the transmission process. When the number of photons in a packet is no more than an integer $v_{th}(v_{th} < \frac{L-1}{2})$, in the analysis of Sasaki et al., the phase error rate can be bounded by $v_{th}/(L-1)$ [8]. While they assume that Eve completely knows the sifted key bits from the rest part($v > v_{th}$).

Zhang et al.[9] improved the phase error estimation by considering the encoding details of the quantum signal. The phase error rate is given by

$$e_{ph}^{n} = \frac{1-(1-2/L)^{n}}{2}. \tag{3}$$

When the number of photons satisfies $v < v_{th}$, phase error rate can be bounded by $\frac{1-(1-2/L)^{v_{th}}}{2}$, which accords a tighter and more reasonable bound on the phase error rate.

Hence, the improved phase error rate estimation of source satisfying $\Pr(v > v_{th}) \leq e_{src}$ is expressed by[8,9]

$$\mathrm{e}_{ph} = \frac{e_{src}}{Q} + (1 - \frac{e_{src}}{Q})\frac{1-(1-2/L)^{\mathrm{v}_{th}}}{2} \tag{4}$$

where Q is the empirical rate of detection $Q = N/N_{em}$, and N_{em} corresponds to the number of packets emitted from Alice. There are $N_{em}e_{src}$ rounds satisfying the number of photons $v > v_{th}$, which are regarded as a phase error in the worst case scenario. So the first term of this equation stands for the fraction of phase error rate where the photons in a packet have exceeded v_{th}, and the second one refers to that of packets whose photons are no larger than v_{th}.

On account of this classification, the secure key rate per packet can be calculated to be[8]

$$R = (Q - e_{src})(1 - f \cdot h(e_{bit}) - h(\frac{1-(1-2/L)^{v_{th}}}{2})) - e_{src} \cdot f \cdot h(e_{bit}). \tag{5}$$

The former part is the contribution of packets containing photons exceeding v_{th}, while the latter one is that of packets containing photons no more than v_{th}. From this equation, it is clear that the larger L is, the higher secure key rate of per packet we can obtain.

Finite decoy-state RRDPS protocol

Decoy-state method[14] has been proposed as a useful method to improve the performance of QKD protocols when using an imperfect single-photon source. Similarly, the decoy-state for RRDPS protocol also have been employed[9]. Here, we review the idea of decoy-state RRDPS.

Denote $Q_{L\mu} = \sum_{n=0}^{\infty} Y_n P_{L\mu}(n)$ to be the overall gain when the source intensity is $L\mu$, and H_{PA} to be the ratio of key rate that is sacrificed in privacy amplification. According to Eq.(2),

the final key rate of per packet can also be written as [9]

$$R = Q_{L\mu}[1 - f \cdot h(e_{bit}) - H_{PA}]. \tag{6}$$

Define Y_n to be the yield of n-photon state, which means the conditional probability of a detection event at Bob side when Alice sends out n-photon state. Note that Y_0 is the background rate, including the detector dark count and other background contributions. Denote $P_\mu(n)$ to be the possibility of n photons when the mean number is μ. The amount of key loss can be calculated as[9]

$$Q_{L\mu}H_{PA} = \sum_{\mathrm{n=0}}^{\infty} Y_n P_{L\mu}(n) h(e_{ph}^n). \tag{7}$$

Y_n cannot be measured directly, but we can accurately estimate it with infinite decoy states. Without the interference of Eve, it is given by[17]

$$Y_n = 1 - (1 - Y_0)(1 - \eta)^n. \tag{8}$$

And the error rate e_n can be obtained from[17]

$$\mathrm{e}_n = \frac{e_0 Y_0 + e_d(1 - Y_0)[1 - (1 - \eta)^n]}{Y_n}. \tag{9}$$

In practice, the number of decoy states cannot be chosen freely. As the number of intensity increases, the enforcement of the protocol may be more challengeable. So it is worthy to study finite decoy-state method. For practical implementations, since contributions from states with large photon numbers are negligible comparing with those from small photon numbers, only a few decoy states will be sufficient. The final key rate can be rewritten as

$$R = \sum_{n=0}^{n_{th}} Y_n P_{L\mu}(n)(1 - f \cdot h(e_{bit}^n) - h(e_{ph}^n)) \tag{10}$$

where Y_n is defined to be the yield of an n-photon state, $P_{L\mu}(n)$ refers to the possibility of n photons when the mean number is $L\mu$, f corresponds to the efficiency of error correction, and $h(e) = -e\log e - (1-e)\log(1-e)$ is the binary Shannon entropy function. n_{th} is the threshold of the photon numbers that are efficient. Define e^n_{bit}, e^n_{ph} to be the bit error rate and phase error rate of n photons respectively. Y_n and e^n_{bit} need to be estimated by using the decoy states method.

In BB84, a protocol with two decoy states, the vacuum and a weak decoy state, only estimating the yield and error rate of single photon, asymptotically approaches the theoretical limit of infinite decoy-state protocol[17]. Since multi-photons are also contributed to the secret key in RRDPS, we propose finite decoy-state to estimate Y_1, Y_2, Y_3 and e_1, e_2, e_3, that is $n_{th} = 3$. Here we set an example of WCPs to show the calculation of these parameters.

Numerical simulation

To describe a practical system, a widely used fiber-based setup model is needed. When the laser source is modeled WCPs, the density matrix of the state can be given by[18]

$$\rho_\mu = \int_0^{2\pi} \frac{d\theta}{2\pi} |\sqrt{\mu}e^{j\varphi}><\sqrt{\mu}e^{j\varphi}| = \sum_{n=0}^{\infty} e^{-\mu}\frac{\mu^n}{n!}|n><n| \tag{11}$$

where $|0><0|$ is the vacuum state and $|n><n|$ is the density matrix of the n-photon state.

HSPS, like the commonly used WCPs, is also within reach of current technology as another candidate of the perfect single-photon source. Given a two-mode state of the form[18]

$$(\cosh\chi)^{-1}\sum_{n=0}^{\infty}(\tanh\chi)^n e^{in\theta}|n,n> \tag{12}$$

Set the intensity of the source μ to $\sinh^2\chi$, then the above description simplifies to[19]

$$\sum_{n=0}^{\infty}\sqrt{\frac{\mu^n}{(1+\mu)^{n+1}}}e^{in\theta}|n,n> . \tag{13}$$

After triggering out one of a photon pair, the other mode is basically a field of distribution[16]

$$p_x = \frac{1}{P_{post}(\mu)}\{\frac{d_A}{1+\mu}|0><0| + \sum_{n=1}^{\infty}[1-(1-\eta_A)^n]\cdot\frac{\mu^n}{(1+\mu)^{n+1}}|n><n|\} \tag{14}$$

where μ is the mean photon number of one mode, η_A , $d_A$account for the detection efficiency and dark count rate of detector respectively. The post-selection probability is$P_{post}(x) = \frac{d_A}{1+x} + \frac{x\eta_A}{1+x\eta_A}$.

Considering the distribution of photons in Eq.11, the gain and QBER for using WCPs can be calculated by[17]

$$Q_{L\mu} = \sum Y_n\frac{(L\mu)^n}{n!}e^{-L\mu} = Y_0 + (1-Y_0)(1-e^{-L\eta\mu}) \tag{15}$$

$$E_{L\mu}Q_{L\mu} = \sum e_nY_n\frac{(L\mu)^{\mathrm{n}}}{(1+L\mu)^{\mathrm{n+1}}} = e_0Y_0 + e_d(1-Y_0)(1-e^{-L\eta\mu}) \tag{16}$$

Based on the formula above, we use the following for the error rate[9]

$$e_{bit} = \frac{E_{L\mu}Q_{L\mu}}{Q_{L\mu}} = \frac{e_0Y_0 + e_d(1-Y_0)(1-e^{-L\eta\mu})}{Y_0 + (1-Y_0)(1-e^{-L\eta\mu})} \tag{17}$$

Denote the loss coefficient in the quantum channel to be α. For an optical-fiber-based system, the relationship between the transmission distance d and the overall transmittance η is[17]

$$d = -\frac{10\log_{10}\eta}{\alpha}. \tag{18}$$

From these formulas, the overall gain and bit error rate for HSPS can be given by

$$Q_{L\mu} = \sum Y_n P_{L\mu}(n)$$

$$= Y_0 \cdot \frac{d_A}{(1+L\mu)\cdot P_{post}(L\mu)} + \sum_{n=1}^{\infty} [1-(1-Y_0)(1-\eta)^n]\cdot[1-(1-\eta_A)^n]\cdot\frac{(L\mu)^n}{(1+L\mu)^{n+1}\cdot P_{post}(L\mu)}$$

$$= \frac{d_A Y_0(1+L\mu\eta_A)+L\mu\eta_A(1+L\mu)}{d_A(1+L\mu\eta_A)+L\mu\eta_A(1+L\mu)} - \frac{L\mu(1-Y_0)(1+L\mu\eta_A)(1-\eta)}{[d_A(1+L\mu\eta_A)+L\mu\eta_A(1+L\mu)](1+L\mu\eta)} \quad (19)$$

$$+\frac{L\mu(1-Y_0)(1+L\mu\eta_A)(1-\eta)(1-\eta_A)}{[d_A(1+L\mu\eta_A)+L\mu\eta_A(1+L\mu)](1+L\mu\eta+L\mu\eta_A-L\mu\eta\eta_A)}$$

$$E_{L\mu}Q_{L\mu} = \sum e_n Y_n P_\mu(n)$$

$$= e_0 Y_0 \cdot \frac{d_A}{(1+L\mu)\cdot P_{post}(L\mu)} + \sum_{n=1}^{\infty} \{[1-(1-\eta)^n]\}\cdot[1-(1-\eta_A)^n]\cdot\frac{(L\mu)^n}{(1+L\mu)^{n+1}\cdot P_{post}(L\mu)}$$

$$= \frac{d_A e_0 Y_0(1+L\mu\eta_A)+L\mu\eta_A(1+L\mu)[e_0Y_0+e_d(1-Y_0)]}{d_A(1+L\mu\eta_A)+L\mu\eta_A(1+L\mu)} \quad (20)$$

$$-\frac{e_d L\mu(1-Y_0)(1+L\mu\eta_A)(1-\eta)}{(d_A(1+L\mu\eta_A)+L\mu\eta_A(1+L\mu))(1+L\mu\eta)}$$

$$+\frac{e_d L\mu(1-Y_0)(1+L\mu\eta_A)(1-\eta)(1-\eta_A)}{(d_A(1+L\mu\eta_A)+L\mu\eta_A(1+L\mu))(1+L\mu\eta+L\mu\eta_A-L\mu\eta\eta_A)}$$

Key rate per packet, R, represents the average net production length of secure key in a fixed length packet. The final asymptotic secret key rate per packet can be given by equation (5). For a fixed length packet, there are optimized mean photon numbers, μ, and thresholds of photons in each packet, v_{th}, in the process of transmission. To clarify the choice of μ and v_{th} intuitionally, we show the relationship among R, μ and v_{th} as following Figure 2. The length of each packet is fixed at 128. The channel transmission is 10^{-5}. By changing values of two variables, we can observe the affect of variables on optimization results of final key rate.

[ht]

Various colors indicate diverse values of key rate per packet. By looking at the graph, all the major values will show up clearly. It is obvious that key rate per packet has a maximum point, where corresponding mean photon number and photons in each packet can be regarded as optimal ones. So in the following simulation we adopt these optimal values for each condition to obtain better key rates.

Let Q be the empirical rate of detection about channel transmission η. For the use of WPCs and HSPS, the key rates per packet with different packet length and bit error rate, as a function of channel transmission, is illustrated in Figure 3. Parameters used are listed in Table 1.

From the results shown in Figure 3, key rates per packet increase as the variation of channel transmission. By simulation, we can see that the key rate or WCPs is mostly larger than that for HSPS when $L = 128$. Two sources perform similarly if L is equal to 64 and $e = 0.03$. When L equals to 32, HSPS performers better. In a word, WCPs is more suitable for larger packet length while HSPS performs better with smaller packet.

According to the distribution of each source, we can obtain the probability of emitting different numbers of photons among WCPs and HSPS. For a better interpretation of this fact, we take a simple comparison in Figure 4.

[ht]

It is apparent that the results of Figure 4 and Figure 3 are coincident as a whole. Roughly

speaking, when $L = 128$, the summation of photons contributing to secure key rate in WCPs is larger than that in HSPS. These two summations are equal to each other while $L = 64$, then the former one is less than the latter one when $L = 32$.

Applying the expressions of $Q_{L\mu}$ and e_{bit} to Eq.5, we can numerically compare the performance of the two sources with decoy-state and without decoy-state. In order to give a faithful estimation, we employ a reasonable model to forecast the result, taking example by a typical QKD system[6]. Here, we fix L at 32, and other parameters used are listed in Table 1.

Combing Eq.6, Eq.7, 8, 9, we can calculate the final key generation rate of RRDPS protocol with and without decoy-state for WCPs and HSPS. For convenience of comparing, we use the same parameters as above in Table 1. Our simulation results are shown in Figure 5.

The decoy-state method is often used to improve the secure key rate and transmission distance in conventional protocol. The simulation result in Figure 5 clearly demonstrates that this method is also effective for the RRPDS protocol. The performance of HSPS is much better than WCPs under these two circumstances.

For the case of WCPs, we compare decoy-state methods for RRDPS protocol with different intensities: infinite decoy states, two-decoy-state method in which we just estimate Y_1 and e_1, three-intensity decoy-state estimating Y_1, Y_2, e_1 and e_2, four-decoy-states estimating Y_1, Y_2, Y_3, e_1, e_2 and e_3.(see the Methods) Then, the comparison between the estimated values and asymptotic values of yields and error rates are shown in Figure 6.

[ht]

From the graph it is evident that the estimated values of yields are infinite approaching the asymptotic values. The estimated error rates are very close to the asymptotic values. Since we have presented partial lower bounds of yield and upper bounds of QBER, we will give an example to show that, even in the case of finite, the performance of our method is close to that of the infinite decoy method. We use the key parameter listed in Table I. Here, we also fix L at 32, and optimize μ to obtain the maximum transmission distance. The simulation result indicates that three decoy states are sufficient for the RRDPS protocol, which is shown in Figure 7.

[ht]

In the decoy-state method of BB84 protocol, only Y_1 and e_1 are needed to estimate, so a few decoy states will be sufficient. This is because contributions from states with large photon numbers are negligible comparing with those from small photon numbers. From the results, we can see that contributions from two-photon state are considerable, while those from three photons are not obvious. Therefore, it is dispensable to estimate yield and QBER when the photon number is more than three.

Discussions

From the comparison between WCPs and HSPS, it is clear that they perform differently with various packet lengths. WCPs is more suitable for larger packet length while HSPS performs better with smaller packet. We anticipate that this result can guide the use of conventional lasers. In current practice, attenuated lasers emitting WCPs are employed in most quantum system. The technology on how to efficiently obtain HSPS has been developed to a high level. It is pragmatic to experimentally test the conclusions from numerical simulations. For practical implementations, we put forward finite decoy-state protocol. Since the key rate of the finite

decoy-state method is close to the infinite one, our protocol can be regarded as a choice for the practical experiment of RRDPS. Taking cost and and technological feasibility into account, our scheme can be promising implementation of quantum cryptography. Compared with existing QKD protocol, there are still many aspects to improve for RRDPS. For example, the finite length of key[20] and its statistical fluctuations can significantly affect the security of RRDPS protocol, which is of special concern.

Methods

Lower bound of Y_1, Y_2, Y_3

Suppose Alice and Bob choose a signal state with intensity $L\mu$ and four decoy states whose intensities are Lv_1, Lv_2, Lv_3, Lv_4, which satisfies

$$Lv_1 \geq Lv_2 \geq Lv_3 \geq Lv_4 \geq 0, L\mu > Lv_1 + Lv_2 + Lv_3 + Lv_4. \tag{21}$$

One can obtain the following gains and quantum bit error rates for the signal and decoy

states

$$
\begin{aligned}
Q_{L\mu}\mathrm{e}^{L\mu} &= \sum_{n=0}^{\infty} Y_n \frac{(L\mu)^n}{n!} & E_{L\mu}Q_{L\mu}e^{L\mu} &= \sum_{n=0}^{\infty} e_n Y_n \frac{(L\mu)^n}{n!} \\
Q_{Lv_1}e^{Lv_1} &= \sum_{n=0}^{\infty} Y_n \frac{(Lv_1)^n}{n!} & E_{Lv_1}Q_{Lv_1}e^{Lv_1} &= \sum_{n=0}^{\infty} e_n Y_n \frac{(Lv_1)^n}{n!} \\
Q_{Lv_2}e^{Lv_2} &= \sum_{n=0}^{\infty} Y_n \frac{(Lv_2)^n}{n!} & E_{Lv_2}Q_{Lv_2}e^{Lv_2} &= \sum_{n=0}^{\infty} e_n Y_n \frac{(Lv_2)^n}{n!} \\
Q_{Lv_3}e^{Lv_3} &= \sum_{n=0}^{\infty} Y_n \frac{(Lv_3)^n}{n!} & E_{Lv_3}Q_{Lv_3}e^{Lv_3} &= \sum_{n=0}^{\infty} e_n Y_n \frac{(Lv_3)^n}{n!} \\
Q_{Lv_4}e^{Lv_4} &= \sum_{n=0}^{\infty} Y_n \frac{(Lv_4)^n}{n!} & E_{Lv_4}Q_{Lv_4}e^{Lv_4} &= \sum_{n=0}^{\infty} e_n Y_n \frac{(Lv_4)^n}{n!}
\end{aligned}
\tag{22}
$$

Given such equations, how can we obtain a tight lower bound on R. This is the main problem for decoy-state protocols.

Based on $v_1 Q_{Lv_2} e^{Lv_2} - v_2 Q_{Lv_1} e^{Lv_1}$, a crude lower bound of Y_0 can be chosen by[17]

$$
Y_0 \geq {Y_0}^L = \max\left(\frac{v_1 Q_{Lv_2} e^{Lv_2} - v_2 Q_{Lv_1} e^{Lv_1}}{v_1 - v_2}, 0\right) \tag{23}
$$

when $Lv_2 = 0$ the equality sign will hold.

By $Q_{Lv_1} e^{Lv_1} - Q_{Lv_2} e^{Lv_2}$, it is clearly that

$$
Q_{Lv_1} e^{Lv_1} - Q_{Lv_2} e^{Lv_2} \leq Y_1 (Lv_1 - Lv_2) + \frac{(Lv_1)^2 - (Lv_2)^2}{(L\mu)^2} (Q_{L\mu} e^{L\mu} - Y_0^L - Y_1 L\mu). \tag{24}
$$

Consequently, we obtain a minimum value of Y_1[17]

$$
Y_1 \geq {Y_1}^L = \frac{\mu}{L(\mu v_1 - \mu v_2 - {v_1}^2 + {v_2}^2)} \left(Q_{Lv_1} e^{Lv_1} - Q_{Lv_2} e^{Lv_2} - \frac{{v_1}^2 - {v_2}^2}{\mu^2} (Q_{L\mu} e^{L\mu} - Y_0^L)\right). \tag{25}
$$

where Y_0^L is the lower bound of Y_0 calculated earlier.

Combine these two equations

$$Q_{Lv_1}e^{Lv_1} - Q_{Lv_2}e^{Lv_2} = Y_1(Lv_1 - Lv_2) + \frac{Y_2}{2!}((Lv_1)^2 - (Lv_2)^2) + \frac{Y_3}{3!}((Lv_1)^3 - (Lv_2)^3) + \cdots \quad (26)$$

$$Q_{Lv_2}e^{Lv_2} - Q_{Lv_3}e^{Lv_3} = Y_1(Lv_2 - Lv_3) + \frac{Y_2}{2!}((Lv_2)^2 - (Lv_3)^2) + \frac{Y_3}{3!}((Lv_2)^3 - (Lv_3)^3) + \cdots \quad (27)$$

With $(Q_{Lv_1}e^{Lv_1} - Q_{Lv_2}e^{Lv_2}) \times (v_2 - v_3) - (Q_{Lv_2}e^{Lv_2} - Q_{Lv_3}e^{Lv_3}) \times (v_1 - v_2)$, we also have

$$(v_2 - v_3)Q_{v_1}e^{v_1} - (v_1 - v_3)Q_{v_2}e^{v_2} + (v_1 - v_2)Q_{v_3}e^{v_3} \leq \frac{Y_2}{2}L^2(v_2 - v_3)(v_1 - v_3)(v_1 - v_2)$$
$$+\frac{(v_2 - v_3)(v_1 - v_3)(v_1 - v_2)(v_1 + v_2 + v_3)}{\mu^3}(Q_{L\mu}e^{L\mu} - Y_0^L - {Y_1}^L L\mu - \frac{Y_2(L\mu)^2}{2}) \quad (28)$$

Therefore, we can bound Y_2 by

$$Y_2 \geq {Y_2}^L = \frac{2\mu[(v_2 - v_3)Q_{Lv_1}e^{Lv_1} - (v_1 - v_3)Q_{Lv_2}e^{Lv_2} + (v_1 - v_2)Q_{Lv_3}e^{Lv_3}]}{L^2(\mu - v_1 - v_2 - v_3)(v_2 - v_3)(v_1 - v_3)(v_1 - v_2)}$$
$$-\frac{v_1 + v_2 + v_3}{(L\mu)^2(\mu - v_1 - v_2 - v_3)}(Q_{L\mu}e^{L\mu} - Y_0^L - {Y_1}^L L\mu) \quad (29)$$

As we have known,

$$(v_2 - v_3)Q_{Lv_1}e^{Lv_1} - (v_1 - v_3)Q_{Lv_2}e^{Lv_2} + (v_1 - v_2)Q_{Lv_3}e^{Lv_3}$$
$$= \frac{Y_2}{2!}L^2(v_2 - v_3)(v_1 - v_3)(v_1 - v_2) + \frac{Y_3}{3!}L^3(v_2 - v_3)(v_1 - v_2)(v_1 - v_3)(v_1 + v_2 + v_3) \quad (30)$$
$$+\frac{Y_4}{4!}L^4(v_2 - v_3)(v_1 - v_2)(v_1 - v_3)({v_1}^2 + {v_2}^2 + {v_3}^2 + v_1v_2 + v_1v_3 + v_2v_3) + \cdots$$

$$
\begin{aligned}
&(v_3-v_4)Q_{Lv_2}e^{Lv_2}-(v_2-v_4)Q_{Lv_3}e^{Lv_3}+(v_2-v_3)Q_{Lv_4}e^{Lv_4}\\
=&\frac{Y_2}{2!}L^2(v_3-v_4)(v_2-v_4)(v_2-v_3)+\frac{Y_3}{3!}L^3(v_3-v_4)(v_2-v_3)(v_2-v_4)(v_2+v_3+v_4)\\
&+\frac{Y_4}{4!}L^4(v_3-v_4)(v_2-v_3)(v_2-v_4)({v_2}^2+{v_3}^2+{v_4}^2+v_2v_3+v_2v_4+v_3v_4)+\cdots
\end{aligned}
\tag{31}
$$

For a similar settlement, we can also give the lower bound of Y_3

$$
\begin{aligned}
Y_3\geq {Y_3}^L=&\frac{3!\mu}{L^3(\mu-v_1-v_2-v_3-v_4)}[\frac{Q_{Lv_1}e^{Lv_1}}{(v_1-v_2)(v_1-v_3)(v_1-v_4)}-\frac{Q_{Lv_2}e^{Lv_2}}{(v_2-v_3)(v_1-v_2)(v_2-v_4)}\\
&+\frac{Q_{Lv_3}e^{Lv_3}}{(v_1-v_3)(v_2-v_3)(v_3-v_4)}-\frac{Q_{Lv_4}e^{Lv_4}}{(v_1-v_4)(v_2-v_4)(v_3-v_4)}]\\
&-\frac{3!(v_1+v_2+v_3+v_4)}{\mu-v_1-v_2-v_3-v_4}\frac{Q_{L\mu}e^{L\mu}-Y_0^L-{Y_1}^LL\mu-\frac{{Y_2}^L(L\mu)^2}{2!}}{(L\mu)^3}
\end{aligned}
\tag{32}
$$

Upper bound of QBER e_1, e_2, e_3

According to the condition, the QBER of decoy state is given by[17]

$$
E_{Lv_1}Q_{Lv_1}e^{Lv_1}=e_0Y_0+e_1Lv_1Y_1+\sum_{n=2}^{\infty}e_nY_n\frac{(Lv_1)^n}{n!} \tag{33}
$$

$$
E_{Lv_2}Q_{Lv_2}e^{Lv_2}=e_0Y_0+e_1Lv_2Y_1+\sum_{n=2}^{\infty}e_nY_n\frac{(Lv_2)^n}{n!} \tag{34}
$$

The upper bound of e_1 can be obtained directly[17]

$$
e_1\leq {e_1}^U=\frac{E_{Lv_1}Q_{Lv_1}e^{Lv_1}-E_{Lv_2}Q_{Lv_2}e^{Lv_2}}{(Lv_1-Lv_2){Y_1}^L} \tag{35}
$$

Combining

$$E_{Lv_1}Q_{Lv_1}e^{Lv_1} - E_{Lv_2}Q_{Lv_2}e^{Lv_2} = e_1Y_1(Lv_1 - Lv_2) \tag{36}$$

$$+\frac{e_2Y_2}{2!}((Lv_1)^2 - (Lv_2)^2) + \frac{e_3Y_3}{3!}((Lv_1)^3 - (Lv_2)^3) + \cdots$$

$$E_{Lv_2}Q_{Lv_2}e^{Lv_2} - E_{Lv_3}Q_{Lv_3}e^{Lv_3} = e_1Y_1(Lv_2 - Lv_3) \tag{37}$$

$$+\frac{e_2Y_2}{2!}((Lv_2)^2 - (Lv_3)^2) + \frac{e_3Y_3}{3!}((Lv_2)^3 - (Lv_3)^3) + \cdots$$

and solving the equality

$$(v_2 - v_3)E_{Lv_1}Q_{Lv_1}e^{Lv_1} - (v_1 - v_3)E_{Lv_2}Q_{Lv_2}e^{Lv_2} + (v_1 - v_2)E_{Lv_3}Q_{Lv_3}e^{Lv_3} \tag{38}$$

$$\geq \frac{e_2Y_2L^2}{2}(v_2 - v_3)(v_1 - v_3)(v_1 - v_2)$$

the upper bound of e_2 can be further represented by

$$e_2 \leq {e_2}^U = \frac{2[(\mathbf{v}_2 - v_3)E_{Lv_1}Q_{Lv_1}e^{Lv_1} - (\mathbf{v}_1 - v_3)E_{Lv_2}Q_{Lv_2}e^{Lv_2} + (v_1 - v_2)E_{Lv_3}Q_{Lv_3}e^{Lv_3}]}{L^2{Y_2}^L(\mathbf{v}_2 - v_3)(\mathbf{v}_1 - v_3)(\mathbf{v}_1 - v_2)} \tag{39}$$

For the same reason, we can obtain the equations followed,

$$(v_2 - v_3)E_{Lv_1}Q_{Lv_1}e^{Lv_1} - (v_1 - v_3)E_{Lv_2}Q_{Lv_2}e^{Lv_2} + (v_1 - v_2)E_{Lv_3}Q_{Lv_3}e^{Lv_3} \tag{40}$$

$$= \frac{e_2Y_2L^2}{2}(v_2 - v_3)(v_1 - v_3)(v_1 - v_2) + \frac{e_3Y_3L^3}{3!}(v_2 - v_3)(v_1 - v_3)(v_1 - v_2)(v_1 + v_2 + v_3) + \cdots$$

$$(v_3 - v_4)E_{Lv_2}Q_{Lv_2}e^{Lv_2} - (v_2 - v_4)E_{Lv_3}Q_{Lv_3}e^{Lv_3} + (v_2 - v_3)E_{Lv_4}Q_{Lv_4}e^{Lv_4} \tag{41}$$

$$= \frac{e_2Y_2L^2}{2}(v_3 - v_4)(v_2 - v_4)(v_2 - v_3) + \frac{e_3Y_3L^3}{3!}(v_3 - v_4)(v_2 - v_4)(v_2 - v_3)(v_2 + v_3 + v_4) + \cdots$$

Then, the upper bound of e_3 can be shown by

$$e_3 \leq {e_3}^U = \frac{3!}{{Y_3}^L L^3}[\frac{E_{Lv_1}Q_{Lv_1}e^{Lv_1}}{(v_1-v_2)(v_1-v_3)(v_1-v_4)} - \frac{E_{Lv_2}Q_{Lv_2}e^{Lv_2}}{(v_2-v_3)(v_1-v_2)(v_2-v_4)} + \frac{E_{Lv_3}Q_{Lv_3}e^{Lv_3}}{(v_1-v_3)(v_2-v_3)(v_3-v_4)} - \frac{E_{Lv_3}Q_{Lv_4}e^{Lv_4}}{(v_1-v_4)(v_2-v_4)(v_3-v_4)}] \tag{42}$$

Acknowledgements

The authors would like to thank Zhen-Qiang Yin and Chun-Mei Zhang for their helpful discussions. This work was supported by the National Basic Research Program of China (Grant No. 2013CB338002) and the National Natural Science Foundation of China (Grants No. 11304397 and No. 61505261).

Author Contributions

Y. Y. Z. presented the theoretical analysis and the numerical simulations and wrote the main manuscript text. C. Z., H. W. L. and Y. W. contributed to the theoretical analysis and discussed the results. W. S. B. and M. S. J. provided essential comments on the manuscript. All authors conceived the research, and commented on the manuscript.

Author Information

The authors declare no competing financial interests.

1. Bennett, C. H. &Brassard, G. Quantum cryptography: Public-key distribution and coin tossing. *IEEE International Conference on Computers, Systems, and Signal Processing* 175-179 (1984).

2. Ekert, A. K. Quantum cryptography based on Bell's theorem. *Phys. Rev. Lett.* **67**, 661 (1991).

3. Lo, H.-K. & Chau, H. F. Unconditional security of quantum key distribution over arbitrarily long distance. *Science* **283**, 2050 (1999).

4. Shor, P. W. & Preskill, J. Simple proof of security of the BB84 quantum key distribution protocol. *Phys. Rev. Lett.* **85**, 441 (2000).

5. Bennett, C. H., Bessette, F., Brassard, G., Salvail, L. & Smolin, J. Experimental quantum cryptography. *Cryptology* **5**, 3 (1992).

6. Gobby, C., Yuan, Z. L. &Shields, A. J. Quantum key distribution over 122 km of standard telecom fiber. *Appl. Phys. Lett.* **84**, 3762 (2004).

7. Bacco, D., Canale, M., Laurenti, N., Vallone, G. & Villoresi, P. Experimental quantum key distribution with finite-key security analysis for noisy channels. *Nature Commun.* **4**, 2363 (2013).

8. Sasaki, T., Yamamoto, Y. & Koashi, M. Practical quantum key distribution protocol without mointoring signal distutbance. *Nature* **509**, 475-478 (2014).

9. Zhang, Z., Yuan, X., Cao, Z. & Ma, X. F. Round-robin differential-phase-shift quantum key distribution. http://arxiv.org/abs/1505.02481 (Accessed on May 11, 2015).

10. Takesue, H., Sasaki, T., Tamaki, K. & Koashi, M. Experimental quantum key distribution without monitoring signal disturbance. *Nature Photon.* **9**, 173 (2015).

11. Wang, S. et al. Experimental demonstration of a quantum key distribution without signal disturbance monitoring. *Nature Photon.* **11**, 209 (2015).

12. Guan, J. Y., Cao, Z. & Liu, Y. Experimental Passive Round-Robin Differential Phase-Shift Quantum Key Distribution. *Phys. Rev. Lett.* **114**, 180502 (2015).

13. Li, Y. H., Cao, Y., Dai, H. & Lin, J. Experimental round-robin differential phase-shift quantum key distribution. http://arxiv.org/abs/1505.08142 (Accessed on May 29, 2015).

14. Hwang, W. Y. Quantum key distribution with high loss: toward global secure communication. *Phys. Rev. Lett.* **91**, 057901 (2003).

15. Lo, H.-K., Ma, X. F. & Chen, K. Decoy state quantum key distribution. *Phys. Rev. Lett.* **94**, 230504 (2005).

16. Wang, X.-B. Beating the photon-number-splitting attack in practical quantum cryptography. *Phys. Rev. Lett.* **94**, 230503 (2005).

17. Ma, X., Qi, B., Zhao, Y. & Lo, H.-K. Practical decoy state for quantum key distribution. *Phys Rev. A* **72**, 012326 (2005).

18. Lütkenhaus, N. Security against individual attacks for realistic quantum key distribution. *Phys. Rev. A* **61**, 052304 (2000).

19. Zhou, C. et al. Tight finite-key analysis for passive decoy-state quantum key distribution under general attacks. *Phys. Rev. A* **89**, 052328 (2014).

20. Ma, X., Fung, C., Boileau, J. C. & Chau, H. F. Universally composable and customizable post-processing for practical quantum key distribution. *Computers & Security* **30**, 172-177 (2011).

Figure 1 Diagram of RRDPS protocol

Figure 2 (Color online) Key rates versus mean photon number and threshold of photons in a packet.

Figure 3 (Color online) Comparison for RRDPS protocol using WCPs and HSPS. The solid curves represent the key rates per packet for using WCPs, the dashed curves stand for key rates for using HSPS. Lines labeled (i)-(iii) characterize the protocol with L=128, 64, 32. The error rate is 0.03 and 0.06, respectively. The choices of v_{th} and the mean photon number μ are optimized.

Figure 4 (Color online) A comparison for the probability of emitting different numbers of photons between WCPs and HSPS. Here parameters for HSPS are listed in Table 1, while the intensity is 0.02 for both WCPs and HSPS.

Figure 5 (Color online) Final key rate without and with decoy states. The solid curves represent the key rates per packet for using WCPs, and the dashed curves stand for key rates for using HSPS. The length of each packet is fixed at 32. The left two curves are the key rates of RRDPS protocol with no decoy states, and the other two are those of the protocol with decoy states.

Figure 6 (Color online) The estimated bounds and asymptotic bounds of yields and error rates. The solid lines represent estimated bounds of yields and error rates, and the dashed lines stand for asymptotic bounds of yields and error rates.

Figure 7 (Color online) Final key rate for using infinite and finite decoy states. The dotted curve accounts for the key rate per packet for infinite decoy-state, and the solid curve stands for the four-intensity decoy-state method to estimate Y_1, Y_2, Y_3, e_1, e_2 and e_3. The dashed curve represents for three-intensity decoy-state method estimating Y_1, Y_2, e_1 and e_2, and the dash-dotted one is on behalf of the two-intensity decoy-state method just estimating Y_1 and e_1. The choices of the mean photon number μ are optimized.

Table 1: Experimental parameters for simulation

η_{A}	d_{A}	e_d	α	f
0.045	1.7×10^{-6}	0.033	0.2dB/km	1.16

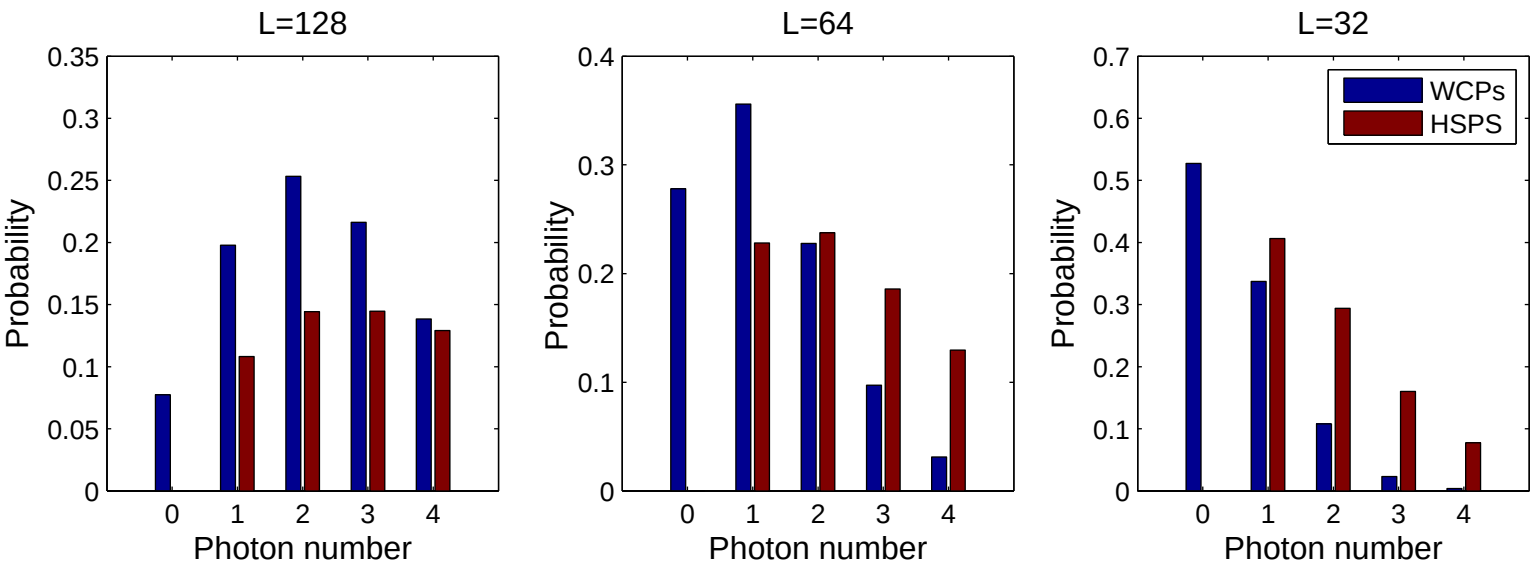
L=128
L=64
L=32
Probability
Photon number
WCPs
HSPS
0
0.05
0.1
0.15
0.2
0.25
0.3
0.35
0.4
0.5
0.6
0.7
1
2
3
4

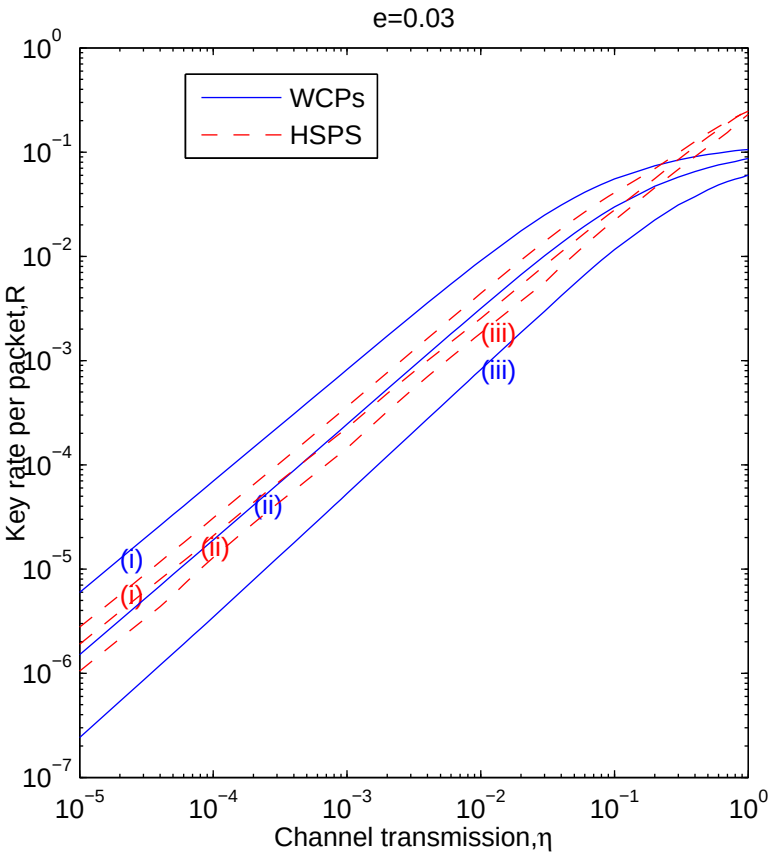
e=0.03
WCPs
HSPS
Key rate per packet,R
Channel transmission,η
(i)
(ii)
(iii)

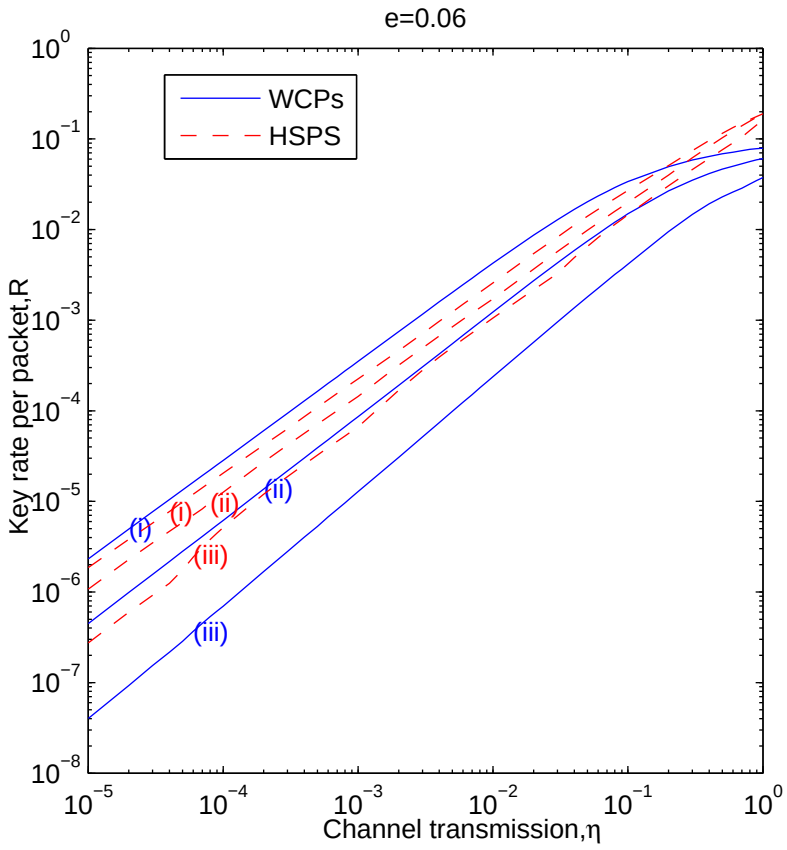
e=0.06
WCPs
HSPS
Key rate per packet,R
Channel transmission,η
(i)
(ii)
(iii)

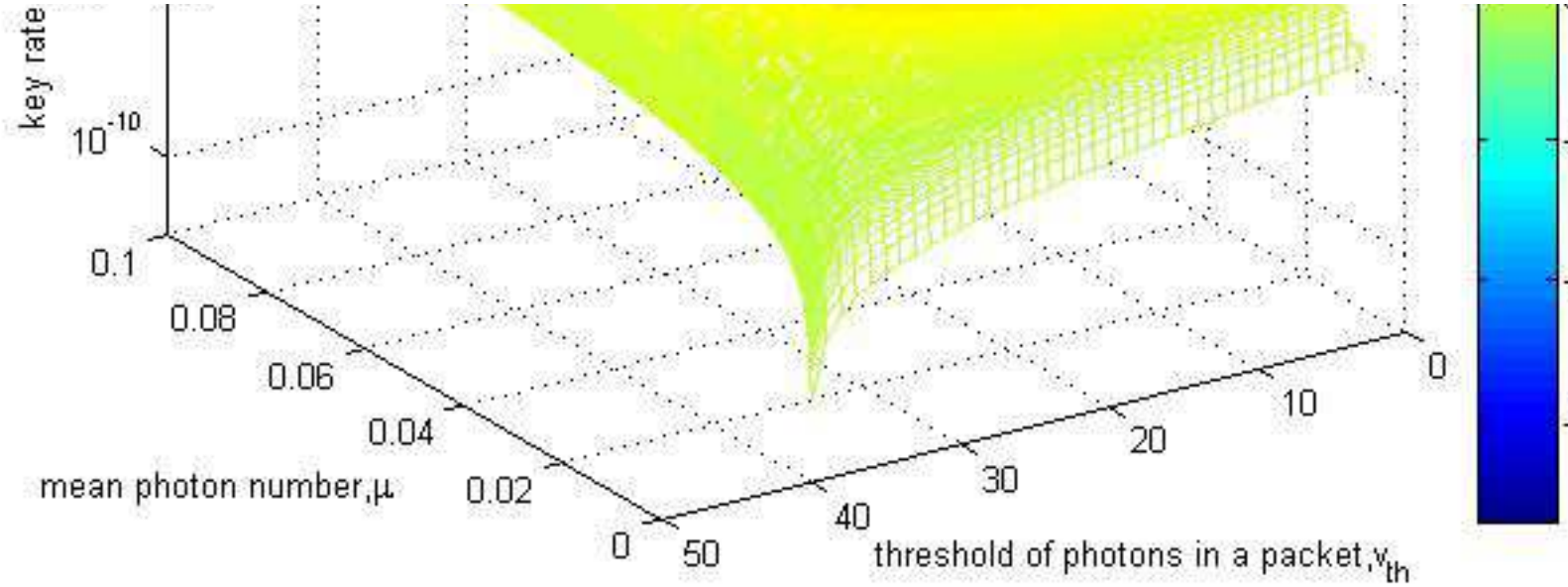
key rate
mean photon number,μ
threshold of photons in a packet,v_th

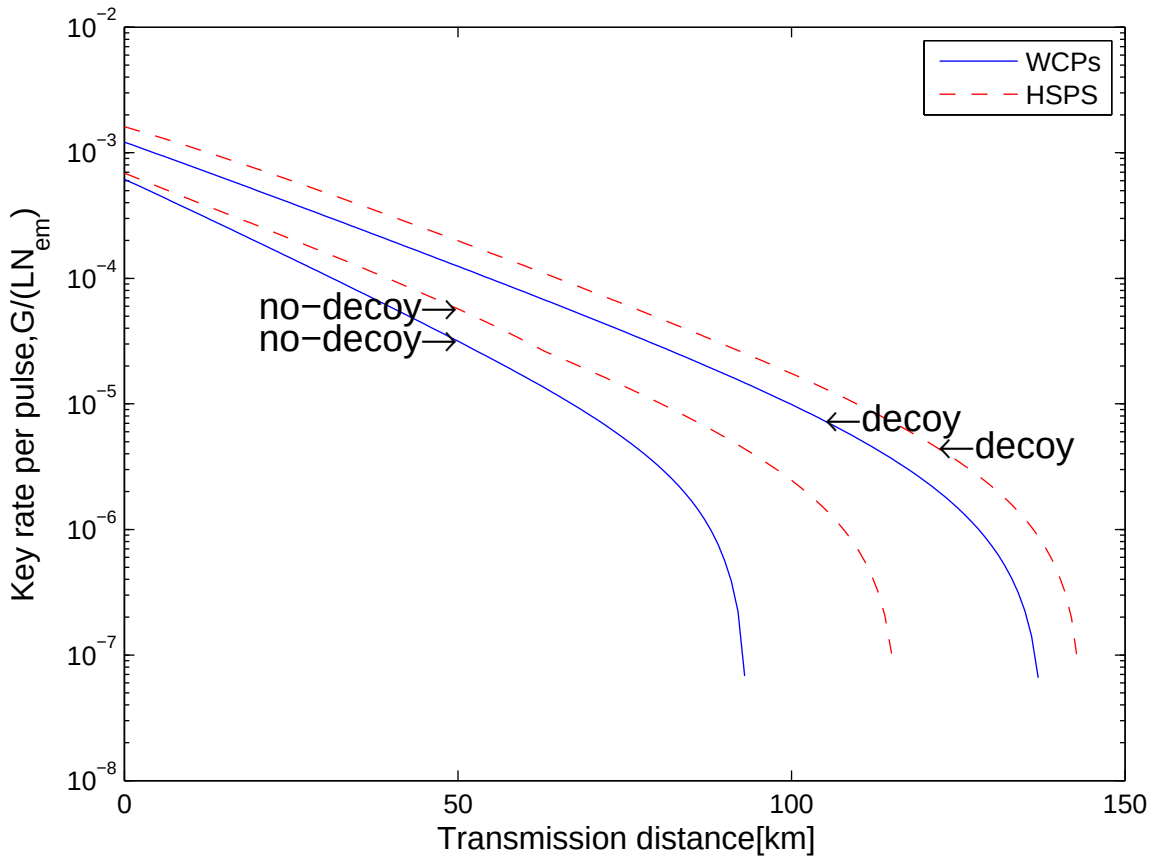
WCPs
HSPS
no−decoy→
no−decoy→
←decoy
←decoy
Key rate per pulse,G/(LN$_{em}$)
Transmission distance[km]
10^{-2}
10^{-3}
10^{-4}
10^{-5}
10^{-6}
10^{-7}
10^{-8}
0
50
100
150

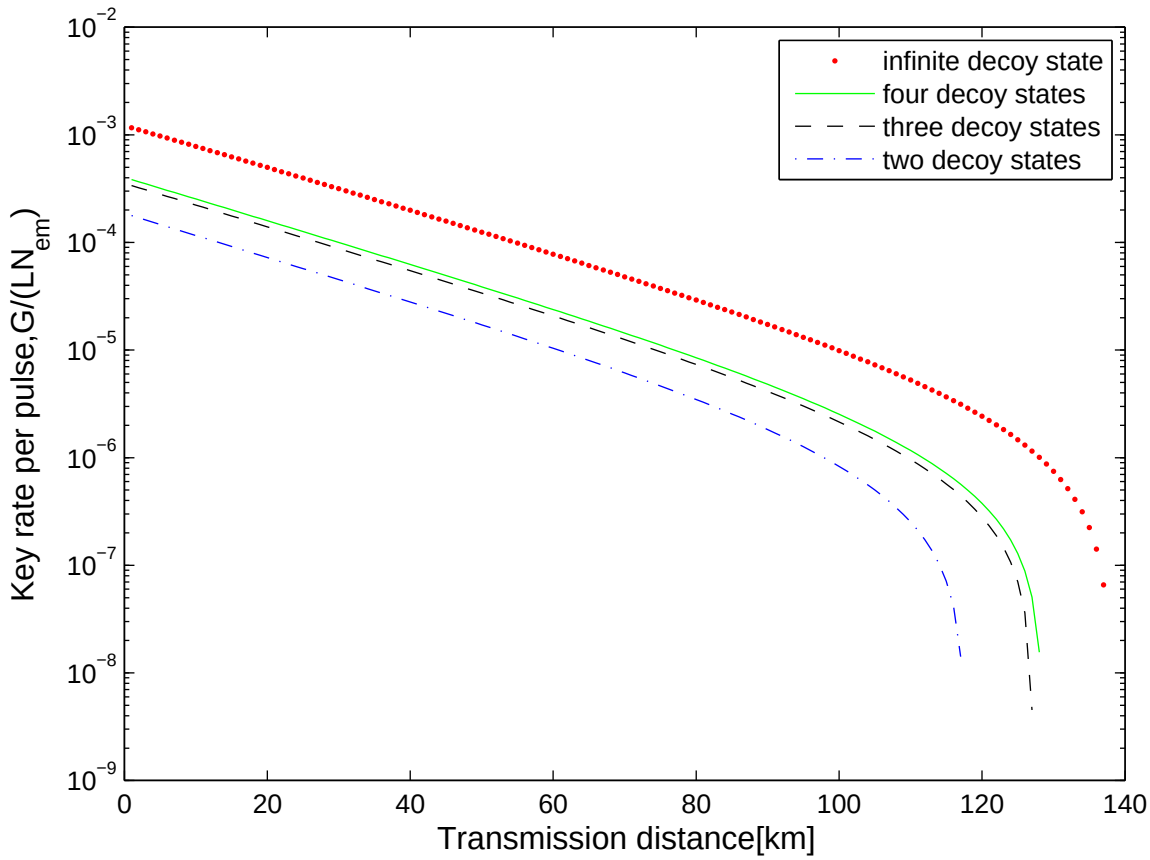
infinite decoy state
four decoy states
three decoy states
two decoy states
Key rate per pulse,G/(LN_em)
Transmission distance[km]
10^-2
10^-3
10^-4
10^-5
10^-6
10^-7
10^-8
10^-9
0
20
40
60
80
100
120
140

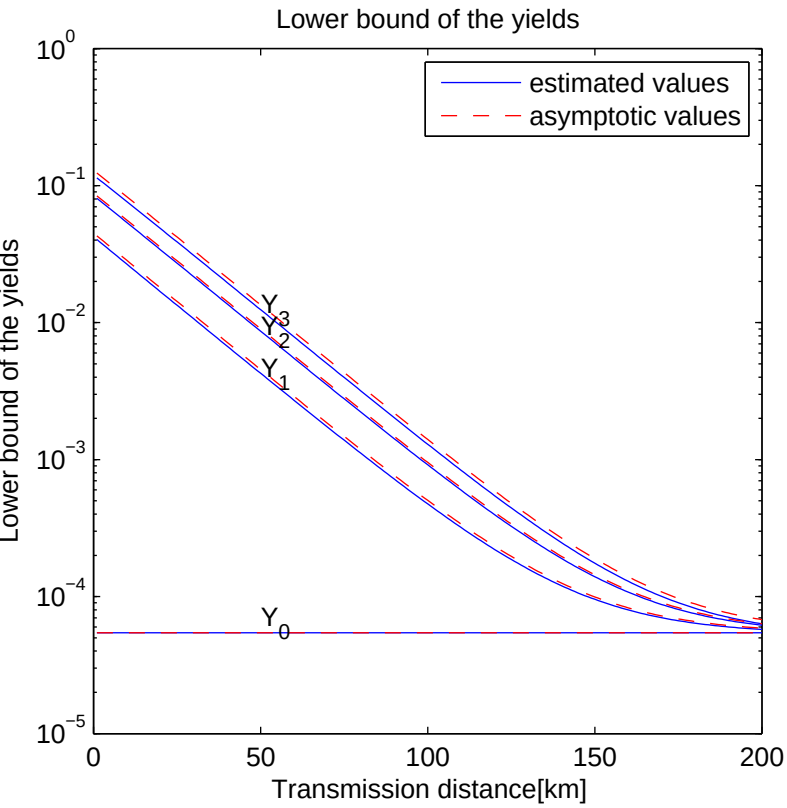
Lower bound of the yields
estimated values
asymptotic values
Lower bound of the yields
Transmission distance[km]
10^{0}
10^{-1}
10^{-2}
10^{-3}
10^{-4}
10^{-5}
0
50
100
150
200
Y_3
Y_2
Y_1
Y_0

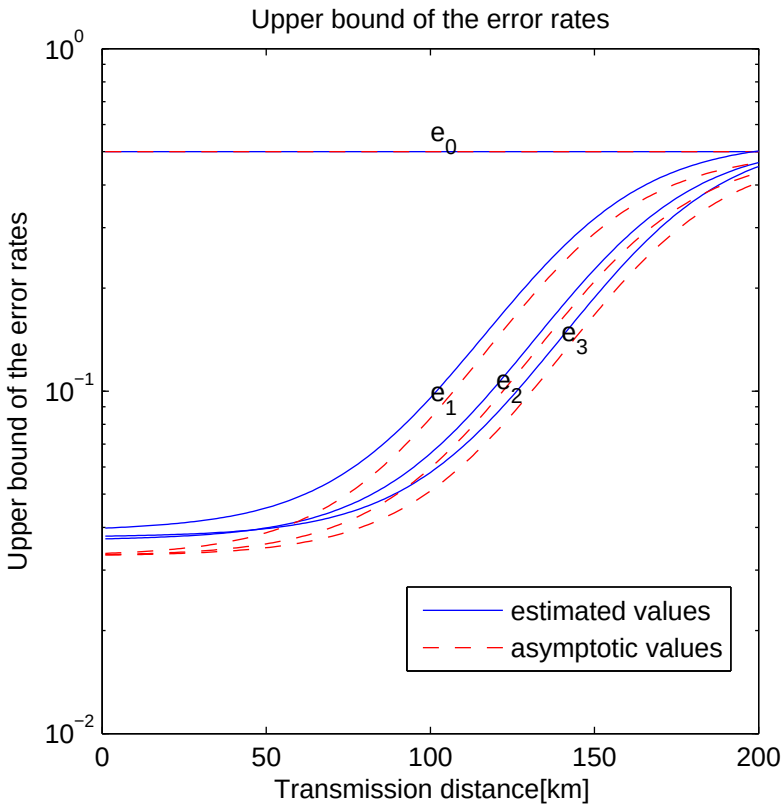
Upper bound of the error rates
Upper bound of the error rates
Transmission distance[km]
10^{0}
10^{-1}
10^{-2}
0
50
100
150
200
e_0
e_1
e_2
e_3
estimated values
asymptotic values